Journal of Photochemistry and Photobiology A: Chemistry 330 (2016) 79–85

Contents lists available at ScienceDirect

Journal of Photochemistry and Photobiology A: Chemistry

journal homepage: www.elsevier.com/locate/jphotochem

Photosensitized production of nitric oxide and peroxynitrite from a carbon-bound diazenium diolate and 2-methyl-2-nitrosopropane

Pedro Sanchez-Cruz, Antonio E. Alegria*

Department of Chemistry, University of Puerto Rico, PO Box 860, Humacao, PR 00792, United States

ARTICLE INFO

Article history:
Received 14 April 2016
Received in revised form 20 July 2016
Accepted 25 July 2016
Available online 27 July 2016

Keywords:
Carbon-bound diazenium diolate
Alanosine
Photosensitization
Oxidation
Nitric oxide
Peroxynitrite
Photodynamic therapy

ABSTRACT

The photosensitized generation of nitric oxide from alanosine (3-(hydroxynitrosoamino)-D,L-alanine) by aluminum phthalocyanine tetrasulfonate (AlPcS4) is reported. While nitric oxide (NO) is obtained in nitrogen-saturated solutions, evidence suggest that both NO and peroxynitrite are produced in air-saturated solutions. Enhancement of NO production occurs in the presence of ubiquinone-0. These observations support the idea that NO is produced by the photosensitized oxidation of alanosine. Both NO and peroxynitrite are detected during photoirradiation of AlPcS4 in the presence of 2-methyl-2-nitrosopropane (MNP) and hypoxanthine (HX), but not in the absence of HX, in air-saturated solutions, thus implying that HX is acting as sacrificial electron donor, thus promoting superoxide formation.

1. Introduction

Nitric oxide (NO) is an endogenously produced molecule that has multiple roles in physiological processes, including angiogenesis, wound healing, neurotransmission, smooth muscle relaxation, and inflammation [1]. Nitric oxide's action on physiology is highly dependent on location, source, and concentration [2]. It is produced in vivo by NO synthase (NOS). Low nanomolar NO concentrations are produced by eNOS and nNOS to promote vasodilation and neurotransmission, respectively [3]. The iNOS form is capable of producing micromolar levels of NO, often responding to infection and inflammation [1]. In the presence of superoxide ($O_2^{\bullet}$), NO will react to form peroxynitrite ($ONOO^-$), an even greater oxidant involved in the inflammatory response [4]. Peroxynitrite causes apoptotic or necrotic cell death through nitration of tyrosine residues in proteins, lipid peroxidation, oxidation of critical thiols, DNA strand breaks, NAD depletion and thus energy failure [5]. NO is also a wound healing promoting agent and, due to its antibacterial activity, it is a promising agent for reducing implant-associated infections and promoting tissue regeneration in orthopedic procedures [6,7].

However, nitric oxide has a short half-life (<1 s) in the presence of oxygen and hemoglobin in vivo, arising from its high reactivity with transition metals and heme-containing proteins [8]. Due to the reactive nature of gaseous NO, its short half-life, instability during storage, and potential toxicity, including its influence on the systemic blood pressure, chemical strategies for NO storage and release have been developed in an effort to use NO's pharmacological potential. Several ways of NO release to tissues have been developed. Diazeniumdiolates (1-amino-substituted diazen-1-ium-1,2-diolate, i.e. NONOates) and S-nitrosothiols represent the two most diverse NO donor classes [9,10]. Other classes are organic nitrates and metal nitrosyl compounds such as sodium nitroprusside and potassium nitrosylpentachlororuthenate [9].

The release of NO from several nanocarriers have been developed to avoid systemic NO side effects while transporting the NO source to the selected tissue [11]. The selective delivery of NO to tissues in adequate concentrations is a developing area of research. These include polymeric nanoparticles, micelles, dendrimers, nanogels, gels, gold nanoparticles, silica nanoparticles and liposomes [11]. The possibility of releasing NO before reaching the tissue site is still a major problem in particle-based systems. In addition, the rate of release of NO at the tissue site using those systems is difficult to be controlled and those where controlled release of NO is observed are mostly metal-based nanoparticle systems containing transition metals with the potential toxicity of those remaining to be tested.

One way of selectively release NO at the needed tissue is to use tissue-penetrating light (wavelengths in the near infrared region, NIR) to activate NO release from molecules. A recent technique,

* Corresponding author.
E-mail address: antonio.alegria1@upr.edu (A.E. Alegria).

http://dx.doi.org/10.1016/j.jphotochem.2016.07.023
1010-6030/

using a 2 photon laser irradiation where NIR photons are added to produce more energetic photons, and NIR-to-visible up-conversion, which are able to release NO from NO-containing molecules and has been developed and used in NO-containing nanoparticles [12–14]. This technique permits the use of longer, tissue-penetrating wavelengths for the photochemical release of NO at the selected tissue site. The use of liposomes for photodelivering NO from NO-containing chromium complexes has also been reported, where NO is detected outside the liposome [15]. However, a non-tissue-penetrating light wavelength was used [15]. The technical problem to overcome is that those photo-controllable NO donors, where all of them contain transition metals, may exhibit systemic toxicity due to release of transition metal ions. In addition, those systems do not generate peroxynitrite, a species which should enhance the toxic activity of NO.

Cupferron, a carbon-bound diazenium diolate, is able to produce nitric oxide photochemically [16] and upon enzymatic oxidation [17]. A natural product with carbon-bound diazenium diolate structure, without the potential carcinogenicity of cupferron [18], is alanosine, Fig. 1. Furthermore, the possibility of generating carcinogenic nitrosamines, as could occur after photolysis of nitrogen-bound diazeniumdiolate ions [19], has not been reported for carbon-bound diazeniumdiolates. Since other NO-containing compounds release NO by photosensitization [20], we were prompted to test the photosensitized generation of NO from this type of compound. In this work we report the photosensitized release of NO from alanosine using NIR radiation. Evidence supports the generation of peroxynitrite from air-saturated dye-alanosine solutions and from air-saturated 2-methyl-2-nitrosopropane (MNP) solutions containing a sacrificial electron donor. Although the photosensitized generation of NO from MNP has been reported previously [20], evidence suggesting the photosensitized production of peroxynitrite by MNP in the presence of the sacrificial electron donor, hypoxanthine (HX), is described here. In the present work we have used MNP to contrast the behavior of alanosine. The photosensitized production of NO could be used in photodynamic therapies of malignancies, where NO or peroxynitrite are used as toxic agents, and where nanoparticle carriers containing both the NO source and the photosensitizer, are transported to the desired tissue.

2. Materials and methods

2.1. Materials

Alanosine 3-(hydroxynitrosoamino)-D,L-alanine, Fig. 1, was obtained from the NCI DTP Repository (Rockville, MD). The dye aluminum phthalocyanine tetrasulfonate (AlPcS4) was purchased from Frontier Scientific. The compounds ubiquinone-0 (UBQ-0), ferricytochrome c, MNP, HX, L-tyrosine, carboxy-PTIO, superoxide dismutase (SOD, from bovine erythrocytes) and 3-nitrotyrosine were purchased from Sigma-Aldrich Co. All solutions were prepared in phosphate buffer and used the same day. Deionized and Chelex-treated water was used in the preparation of all stock and sample solutions. Chelex treatment of water and buffer was monitored using the ascorbate test, as described by Buettner [21]. Care was always taken to minimize exposure of solutions to light.

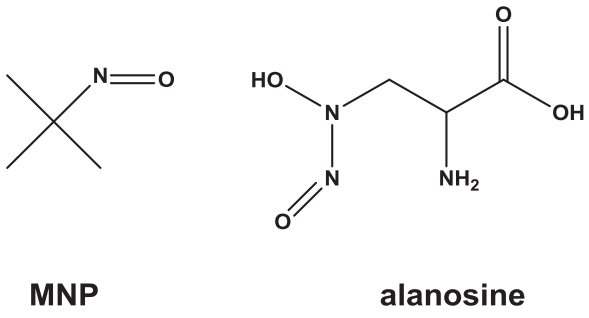

Fig. 1. Alanosine and MNP structures.

2.2. Methods

2.2.1. Sample irradiation for EPR analysis

The NO probe, carboxy-PTIO, was used to detect NO formation from the production of the carboxy-PTI EPR spectrum, as reported previously [22–24]. Air- or N_2-saturated samples containing AlPcS4 (with absorbance of 1 at 675 nm), alanosine (or MNP, in the presence and absence of HX), in the presence or absence of ubiquinone-0 and carboxy-PTIO in 50 mM phosphate buffer (pH 7.4) were irradiated at 675 nm in a 1 cm light path Pyrex cuvettes with continuous stirring for different periods of time. At the end of each period, samples were then transferred into N_2- or air-saturated EPR flat quartz cells ($60 \times 10 \times 0.25$ mm) and placed in the EPR instrument cavity for analysis. A 1000 W xenon arc lamp coupled to a Spectral Energy GM 252 high-intensity grating monochromator with a bandwidth of ± 20 nm was used as the irradiation source. EPR spectra were recorded on a Bruker ER-200D spectrometer at 100 kHz magnetic field modulation. EPR line intensities were determined from the peak-to-peak derivative amplitudes times the square of the peak-to-peak widths.

2.2.2. Sample irradiation in the NO electrode chamber

Nitric oxide production rates were monitored using a NO-specific electrochemical probe (ISO-NOP) inserted in a thermostated NO chamber (World Precision Instruments, Sarasota, FL) at 37 °C. The chamber was either saturated with air or purged with high purity nitrogen followed by injection of 1.00 mL of an air- or nitrogen-saturated solution containing from 0 to 1 mM alanosine or 0–3 mM MNP, 10 μM AlPcS4 and 0 or 500 μM UBQ-0 in 50 mM phosphate buffer (pH 7.4). This was followed by immediate exclusion of all gas bubbles out of the sample, through the chamber capillary. The sample was continuously stirred using a spinning bar. Data acquisition was started before irradiation. The sample was then irradiated at 670 nm using a B&W Tek diode laser with a constant power of 255 mW. Basal voltage was calibrated to zero every day. Voltage output corresponding to a 20 μM NO solution was checked every day, and the electrode membrane was replaced in case there was no agreement with previous outputs within 10%. The electrode was calibrated daily with known concentrations of $NaNO_2$ by reacting this salt with KI in sulfuric acid medium. NO production data were collected in a computer, and the initial rates of NO consumption (RNO) were measured. RNO values reported are averages of 3 determinations for each type of sample.

2.2.3. Peroxynitrite formation

Peroxynitrite formation was detected indirectly by its reaction with L-tyrosine to produce 3-nitrotyrosine, as described previously [25]. For this purpose, micromolar amounts of L-tyrosine were included in the air-saturated samples to be irradiated and its nitro-substituted product detected at 274 nm using HPLC. HPLC analyses were performed using a HP Zorbax SB-C18 (4.6×250 mm) column and eluted with a solvent mixture of 95% ammonium acetate (pH 4.7) and 5% methanol. An Agilent 1100 analytical HPLC system with absorption detection at 276 nm and a flow rate of 0.8 mL/min was used. The retention times of L-tyrosine and 3-nitrotyrosine peaks were determined using commercial standards. All determinations were repeated at least three times, and the average of these determinations is reported.

2.2.4. Superoxide production

Superoxide production was measured using the SOD-inhibitable ferricytochrome c reduction method, as described elsewhere [26,27]. Air-saturated solutions containing 0 or 1 mM HX, 10 μM AlPcS4 and 50 μM ferricytochrome C were irradiated at 675 nm for 10 min followed by measuring the solution absorbance at 550 nm. The latter was performed in the presence and absence of 100 U/mL of SOD. Differences in absorbances of irradiated solutions in the presence and absence of SOD correspond to the SOD-inhibitable absorbances. The latter are proportional to the superoxide concentration produced.

3. Results and discussion

3.1. Photoirradiation of alanosine-containing solutions

Photoirradiation, at 675 nm, of a N_2-saturated sample, containing 4 mM carboxy-PTIO, 10 μM AlPcS4, 500 μM alanosine and 50 mM phosphate buffer (pH 7.4) produces the NO-derived carboxy-PTI EPR spectrum, Fig. 2 b), indicating the photosensitized production of NO. Carboxy-PTIO and carboxy-PTI spectra are characterized by splitting constants aN (2Ns) = 8.10 G and g value = 2.0062 for carboxy-PTIO and aN (1N) = 9.8 G, aN (1N) = 4.4 G and g value = 2.0059 for carboxy-PTI, in agreement with reported values [28,29]. The lowest field EPR peak of carboxy-PTI increases in intensity as a function of irradiation time, Fig. 3. If an identical sample is saturated with air, a smaller intensity of the lowest-field carboxy-PTI EPR peak is detected as compared to that corresponding to the N_2-saturated sample, after 15 min of irradiation, Fig. 2 d) vs b). This indicates that oxygen is competing against alanosine in reacting with the dye excited state. In a previous work we reported that the quinone 2,5-dichloro-diaziridinyl-1,4-benzoquinone enhances the photosensitized oxidation of HX by, presumably, inhibiting back electron transfer from the reduced dye to the HX cation [30]. Thus we tested if UBQ-0 presents a similar behavior in the present system by enhancing alanosine photosensitized oxidation. In fact, addition of 500 μM UBQ-0 to an air-saturated solution of alanosine with the same composition as described above increases the intensity ratio of the lowest-field EPR peak of carboxy-PTI to that of the lowest-field EPR peak of carboxy-PTIO by a factor of 2, Fig. 2 d) vs e). An increase by a factor of ca. 3.5 in the same ratio of peak intensities is detected, upon 500 μM UBQ-0 addition, in N_2-saturated solutions, Fig. 2 b) vs c). The larger increase in carboxy-PTI production upon UBQ-0 addition under N_2- vs air-saturated conditions should be due to the absence of oxygen competition for both the excited and reduced

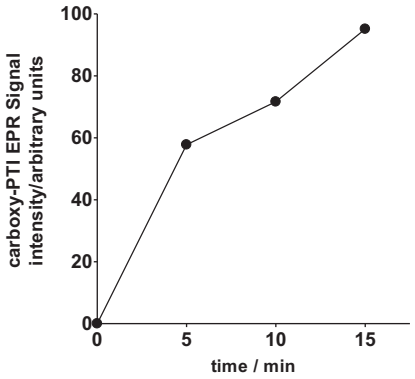

Fig. 3. Increase in the lowest-field EPR peak intensity of carboxy-PTI with irradiation time at 675 nm of a N_2-saturated sample containing 500 μM carboxy-PTIO, 500 μM alanosine, AlPcS4 (A = 1) and 50 mM phosphate buffer (pH = 7.4).

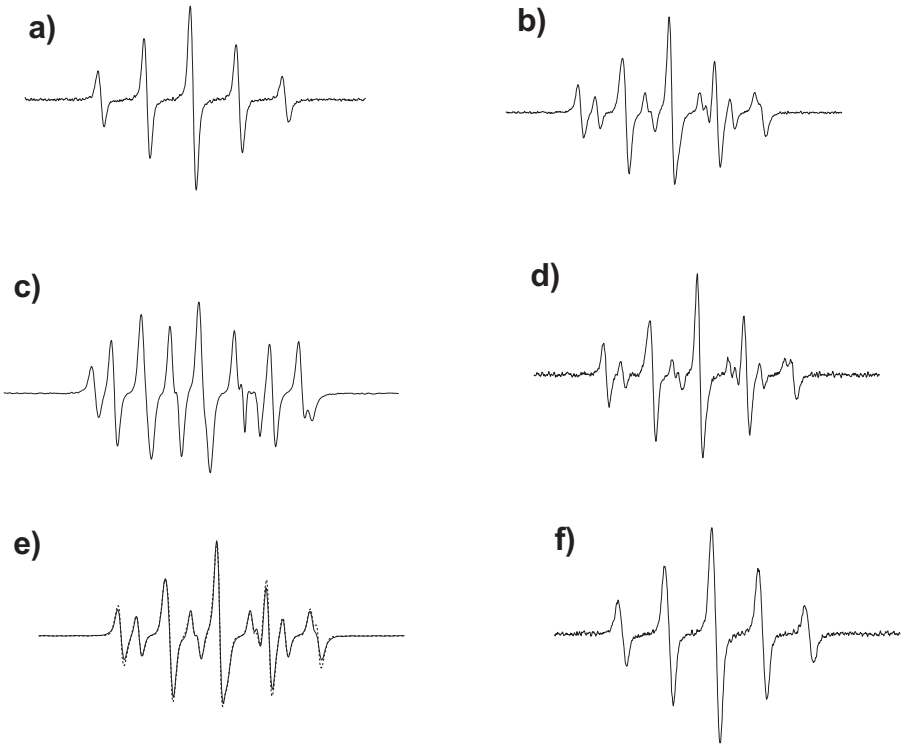

Fig. 2. EPR spectra obtained after 15 min irradiation at 675 nm of samples containing 0 or 1 mM alanosine, 0 or 10 μM AlPcS4, 500 μM carboxy-PTIO in 50 mM phosphate buffer (pH 7.4). Specific additional conditions of each sample are: (a) 0 mM alanosine, 10 μM AlPcS4, N_2-saturated; (b) 1 mM alanosine, 10 μM AlPcS4, N_2-saturated sample; (c) 1 mM alanosine, 10 μM AlPcS4, N_2-saturated sample + 500 μM UBQ-0; (d) 1 mM alanosine, 10 μM AlPcS4, air-saturated sample; (e) 1 mM alanosine, 10 μM AlPcS4, air-saturated sample + 500 μM UBQ-0; (f) 1 mM alanosine, 0 μM AlPcS4, N_2-saturated sample. Dotted-line spectrum in (e) corresponds to a spectral simulation and optimization using WINSIM with parameters stated in Results and Discussion [34].

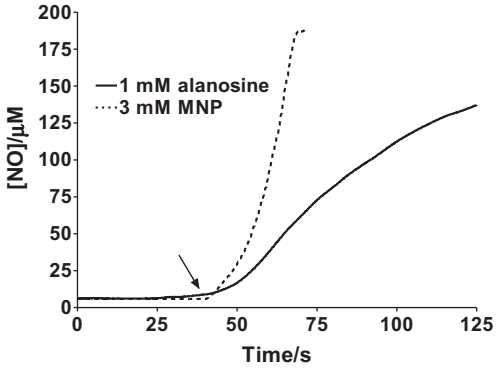

Fig. 4. NO traces after illumination at 670 nm of N_2-saturated samples containing 1 mM alanosine or 3 mM MNP in the presence of 10 μM AlPcS4 and 50 mM phosphate buffer (pH 7.4) at 37 °C. Arrow indicates the instance illumination is started.

dye in N_2-saturated solutions. No carboxy-PTI is observed in the absence of alanosine or dye, Fig. 2 a) and f). The observations stated above suggest that a photosensitized oxidation of alanosine is occurring since: (a) a similar behavior, i.e. quinone-induced enhancement of the anaerobic photosensitized oxidation of HX by AlPcS4 was observed previously [30] (b) enzymatic oxidation of carbon-bound diazenium diolates produces NO [17] and (c) the UBQ-0 semiquinone is detected.

Further evidence for the photosensitized production of NO was obtained by the photoirradiation of a solution containing 1 mM alanosine, 10 μM AlPcS4 and 50 mM phosphate buffer (pH 7.4) under air- or N_2-saturated conditions at the NO electrode chamber, Fig. 4. Again, rates of NO formation are smaller in air- as compared to N_2-saturated conditions, Table 1. Furthermore, addition of 500 μM UBQ-0 to air-saturated or N_2-saturated solutions increases the rate of NO formation by ca. 12.3 and ca. 3.3, respectively, Table 1. Evidence that electrons are being provided to UBQ-0, via the reduced species of the dye, by alanosine oxidation, is the appearance of the semiquinone of UBQ-0 in N_2-saturated solutions and only when both dye and alanosine are present in the irradiated sample, Fig. 5.

Scheme 1 depicts a possible mechanism supported by these observations. Light absorbtion by the dye generates the excited singlet state of the dye which rapidly undergoes intersystem crossing to the dye triplet state (Dye*). In the presence of oxygen singlet oxygen ($^1O_2$, Type II pathway) and the superoxide ion ($O2^{\bullet-}$, Type I pathway) are generated. Another Type I pathway, which could occur exclusively in the absence of oxygen, is the oxidation of alanosine by the excited dye (reaction [4]). UBQ-0 will accept electrons from the reduced dye reaction [5] followed by semiquinone disproportionation (reaction [6]), thus inhibiting back-electron transfer (reverse of reaction [4]). Since the UBQ-0

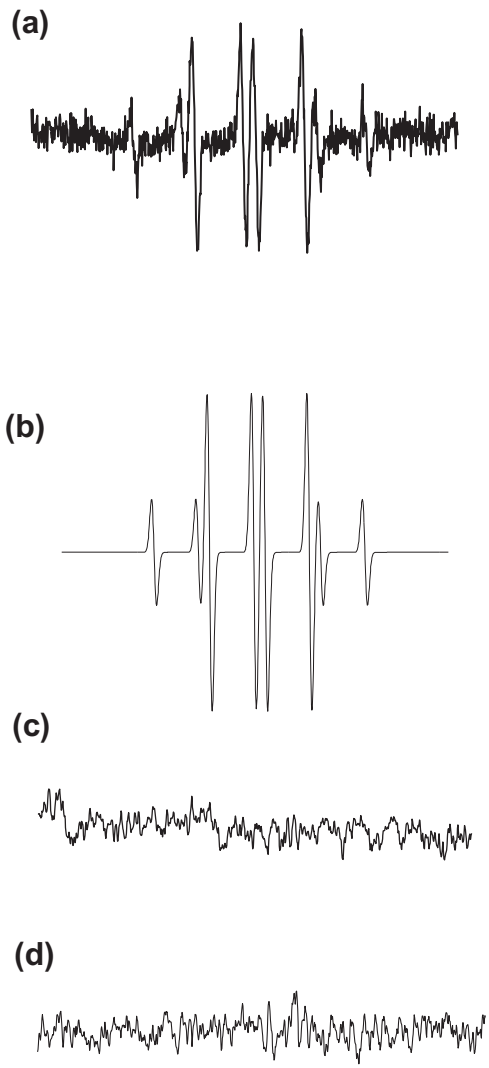

Fig. 5. Epr spectra corresponding to irradiated N_2-saturated solutions at 670 nm containing 50 mM phosphate buffer (pH 7.4), (a) 10 μM AlPcS4, 1 mM alanosine and 500 μM UBQ-0, (c) 10 μM AlPcS4, 0 mM alanosine and 500 μM UBQ-0, (d) 0 μM AlPcS4, 1 mM alanosine and 500 μM UBQ-0. Spectrum (b) is a spectral simulation and optimization using WINSIM. Hyperfine coupling constants are aH(3Hs) = 2.44 G, aH(1H) = 1.95 G and aH(6Hs) = 0.03 G, which agree with previously reported values [35].

concentration used (500 μM) should be much higher than the steady state concentrations of both the intermediate species R-Dye and alanosine$^{\bullet+}$, a high probability for reaction [5] to occur, in competition against reverse of reaction [4], is expected. Thus, UBQ-0 reduction by the reduced dye could explain while UBQ-0

Table 1
Initial rates of NO formation, RNO, under several conditions, in irradiated samples at 675 nm containing 1.0 mM alanosine or 3.0 mM MNP, 10 μM $AlPcS_4$, 50 mM phosphate buffer (pH 7.4) and the stated conditions. Errors are the standard deviations of the average of 3 determinations.

NO source	N_2-saturated	air-saturated	RNO (μM/s)	RNO_{+UBQ}/RNO_{-UBQ}[a]
alanosine	X		2.03 ± 0.03	3.3
	+500 μM UBQ-0		6.8 ± 0.2	
		X	0.12 ± 0.03	12.3
		+500 μM UBQ-0	1.47 ± 0.04	
MNP	X		2.4 ± 0.2	1.2
	+500 μM UBQ-0		2.8 ± 0.1	
		X	0.51 ± 0.05	1.3
		+500 μM UBQ-0	0.67 ± 0.04	

[a] Ratio of RNO in the presence of UBQ-0 to that in its absence.

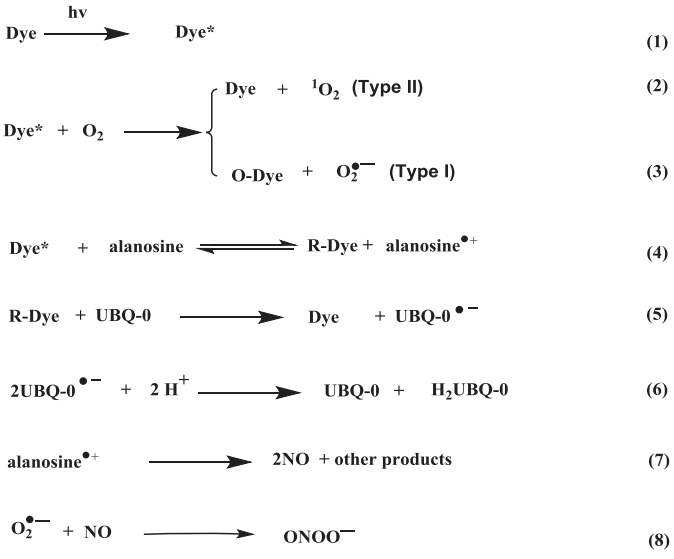

Scheme 1. Proposed mechanism for the photosensitized oxidation of alanosine and its enhancement by UBQ-0, where H_2UBQ-0 is the ubiquinone hydroquinone. The dye is a tetraanionic species. The species R-Dye and O-Dye represents reduced and oxidized species of the dye, respectively.

increases NO production in the case of alanosine-containing samples. However, while the experimental observations plausibly support the alanosine photosensitized oxidation, these are not enough to rule out other possibilities. Further work regarding the identification of other intermediates and products will aid in establishing a more conclusive pathway.

The bimolecular rate constant for the reaction of alanosine with the excited sensitizer (k_4, see Scheme 1) is a measure of the ability of the sensitizer to produce NO from alanosine and can be determined as described previously by Singh et al. [20], assuming a competition between alanosine and O_2 in colliding with the excited dye in air-saturated solutions. If the initial rate of NO formation in air-saturated solutions at a given alanosine concentration (RNO) is measured and compared to the limiting initial rate at saturating alanosine concentration $(RNO)_{max}$, the following equation is obeyed:

$$\frac{1}{RNO} = \frac{k_{O_2}[O_2]}{k_4[\text{alanosine}](RNO_{max})} + \frac{1}{RNO_{max}} \quad (9)$$

where k_{O2} and k_4 are the bimolecular rate constants between the excited state of AlPcS4 and 0_2 and alanosine, respectively. The rate constant, k_{O2}, when the dye is AlPcS4, has been reported as $1.8 \times 10^9\ M^{-1}\ s^{-1}$ [31]. Thus, the bimolecular rate constant k_4 can be determined from the slope of the plot of 1/RNO vs 1/[alanosine], Fig. 6. From the slope and intercept of that graph, the concentration of oxygen and k_{O2}, a value of $k_4 = (4.2 \pm 0.3)$ x $10^8\ M^{-1}\ s^{-1}$ is obtained.

3.2. Photosensitized peroxynitrite production in alanosine-containing solutions

Photoirradiation of an air-saturated sample containing 10 μM AlPcS4, 2.0 mM alanosine, 100 μM tyrosine and 50 mM phosphate buffer (pH 7.4) produces 3-nitrotyrosine, as identified by HPLC using a commercial standard, Table 2. The latter is indirect evidence for peroxynitrite formation [32]. Thus, the reaction of the photosensitized generation of superoxide ($O_2^{\bullet-}$) with NO produces the powerful oxidant and nitrating agent, peroxynitrite ($ONOO^-$).

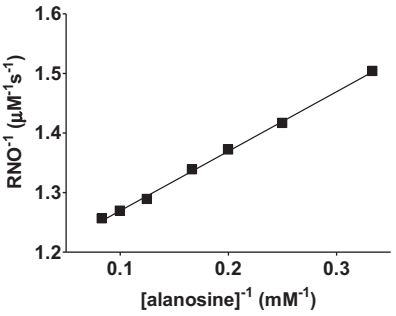

Fig. 6. Determination of k_4 for alanosine. Air saturated samples containing 10 μM AlPcS4, alanosine in 50 mM phosphate buffer (pH 7.4) were irradiated at 670 nm in the NO electrode chamber and initial NO rates were determined from the NO traces.

Table 2
Amounts of 3-nitrotyrosine obtained after photolysis at 675 nm of air-saturated samples containing AlPcS4 (A = 1 at 675 nm), alanosine or MNP, 100 μM L-tyrosine and 50 mM phosphate buffer (pH 7.4). Errors are the standard deviations of the average of 3 determinations.

NO source	Irradiation time/min	[HX]/mM	[3-nitrotyrosine]/μM
2 mM alanosine	10	0	5 ± 1
	15	0	11 ± 2
	20	0	16 ± 3
2 mM MNP	10	1	0
	15	1	0
	25	1	0.5 ± 0.1

3.3. Photoirradiation of MNP-containing solutions

The photosensitized release of NO by MNP solutions in the presence of AlPcS4 has been reported previously [20] and reproduced here, Fig. 4. Energy transfer from the triplet state of AlPcS4 to the triplet state of MNP was postulated to lead to the enhanced homolytic decomposition of MNP to generate NO and the *tert-butyl* radical. Since MNP photosensitized oxidation is not the pathway for NO release from MNP, UBQ-0 addition to MNP-containing solutions has no such dramatic effect on the rate or extent of the photosensitized NO release from MNP, Table 1. No 3-nitrotyrosine formation was detected in air-saturated samples containing MNP and AlPcS4, even after 25 min of irradiation. In a previous work, we observed that a sacrificial electron donor such as HX enhances the AlPcS4-photosensitized reduction of an electron acceptor such as an alkylating quinone, via HX photosensitized oxidation [30]. In another work we also reported that xanthine (the 2-electron oxidation product of HX) enhances the AlPcS4 photosensitized reduction of oxygen [33]. Thus, we hypothesized in the present work that addition of HX to an air-saturated MNP-containing solution should enhance oxygen reduction with the consequent production of superoxide and, therefore, peroxynitrite should be detected. In fact, if HX is added to MNP + AlPcS4 solutions, 3-nitrotyrosine is detected after 25 min of irradiation although in much smaller amounts than that detected for alanosine + AlPcS4 solutions at an even shorter period of irradiation, and with identical MNP and dye concentrations as those used in alanosine-containing solutions, Table 2. That HX enhances the photosensitized production of superoxide is proven by our measurement of the SOD-inhibitable reduction of ferricytochrome C. Addition of 1.0 mM HX to an air-saturated solution containing 10 μM AlPcS4 and 50 μM ferricytochrome C in 50 mM phosphate buffer (pH 7.4), which was irradiated for 10 min at 670 nm, produces an increase by a factor of 2.9 (0.058 ± 0.002 vs 0.020 ± 0.001) in the SOD-inhibitable absorbance at 550 nm. Thus,

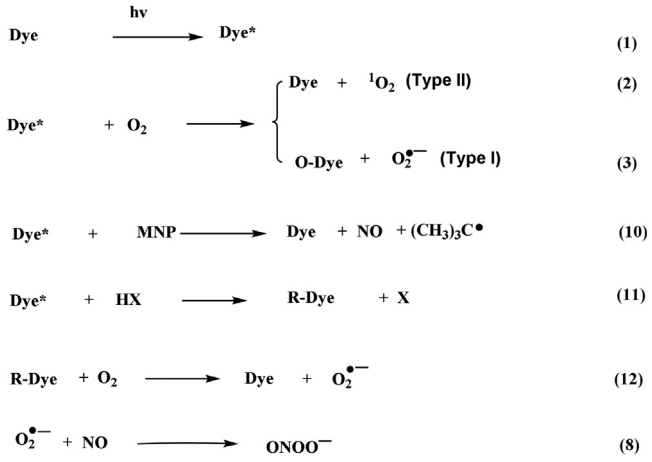

Scheme 2. Proposed mechanism for the photosensitized release of NO from MNP, where X is xanthine. The dye is a tetraanionic species. The species R-Dye and O-Dye represents reduced and oxidized species of the dye, respectively.

HX is providing the electrons for the increase in superoxide production, and thus in peroxynitrite formation. Scheme 2 accounts for this observation. Reaction [10] in this Scheme has been previously reported by Singh et al. [20] as the reaction responsible for NO production. Reactions [11,12,8], account for HX photosensitized oxidation, oxygen reduction and peroxynitrite formation, respectively.

The fact that alanosine requires no additional sacrificial electron donor to produce peroxynitrite, while MNP does, further supports the idea that NO is released from alanosine through the alanosine photosensitized oxidation pathway. In contrast to alanosine, addition of UBQ-0 to MNP-containing solutions has no significant effect on the extent of the photosensitized NO production, since the mechanism of NO release by MNP is not oxidation [20].

4. Summary

The photosensitized production of NO from alanosine occurs under aerobic and anaerobic conditions. While the presence of UBQ-0 increases the rate of photosensitized NO production by alanosine, with the consequent production of the UBQ-0 semi-quinone under anaerobic conditions, it has little influence on the rate of photosensitized production of NO by MNP. These observations suggest that NO is produced by the photosensitized oxidation of alanosine. In air-saturated solutions, AlPcS4 photo-sensitize the production of peroxynitrite from alanosine while the photosensitized production of peroxynitrite from MNP requires the presence of HX as sacrificial electron donor. This work demonstrates that a carbon-bound diazenium diolate such as alanosine can be photosensitized to produce both NO and peroxynitrite. The photosensitized production of NO could be used in photodynamic therapies of malignancies where NO or peroxynitrite are used as toxic agents and where nanoparticle carriers, containing both the NO source and the photosensitizer, are transported to the desired tissue.

Acknowledgments

The authors are grateful to the Puerto Rico Science and Technology Trust for the support of this work (grant # 2015-00046) and to the NCI Developmental Therapeutics Program (http://dtp.cancer.gov) for providing alanosine samples.

References

[1] A.W. Carpenter, M.H. Schoenfisch, Nitric oxide release: part II: therapeutic applications, Chem. Soc. Rev. 41 (2012) 3742–3752.
[2] D.L.H. Williams, A chemist's view of the nitric oxide story, Org. Biomol. Chem. 1 (2003) 441–449.
[3] C. Feng, Mechanism of nitric oxide synthase regulation: electron transfer and interdomain interactions, Coord. Chem. Rev. 256 (2012) 393–411.
[4] P. Codoñer-Franch, V. Valls-Bellés, A. Arilla-Codoñer, E. Alonso-Iglesias, Oxidant mechanisms in childhood obesity: the link between inflammation and oxidative stress, Transl. Res. 158 (2011) 369–384.
[5] P. Calcerrada, G. Peluffo, R. Radi, Nitric oxide-derived oxidants with a focus on peroxynitrite: molecular targets, cellular responses and therapeutic implications, Curr. Pharm. Des. 17 (2011) 3905–3932.
[6] G. Han, L.N. Nguyen, C. Macherla, Y. Chi, J.M. Friedman, J.D. Nosanchuk, L.R. Martinez, Nitric Oxide-releasing nanoparticles accelerate wound healing by promoting fibroblast migration and collagen deposition, Am. J. Pathol. 180 (2012) 1465–1473.
[7] S.P. Nichols, W.L. Storm, A. Koh, M.H. Schoenfisch, Local delivery of nitric oxide: targeted delivery of therapeutics to bone and connective tissues, Adv. Drug Deliv. Rev. 64 (2012) 1177–1188.
[8] L. Ignarro, Nitric Oxide: Biology and Pathobiology, Academic San Diego, Calif, 2000.
[9] J. Kim, G. Saravanakumar, H.W. Choi, D. Park, W.J. Kim, A platform for nitric oxide delivery, J. Mater. Chem. B 2 (2014) 341–356.
[10] J.A. Hrabie, L.K. Keefer, Chemistry of the nitric oxide-releasing diazeniumdiolate (nitrosohydroxylamine) functional group and its oxygen-substituted derivatives, Chem. Rev. 102 (2002) 1135–1154.
[11] J. Saraiva, S. Marotta-Oliveira, S. Aparecida, J. de-Oliveira, J. Maldonado, Nanocarriers for nitric oxide delivery, J. Drug Deliv. 2011 (2011) 1–16.
[12] J. Cao, S. Huang, Y. Chen, S. Li, X. Li, D. Deng, Z. Qian, L. Tang, Y. Gu, Near-infrared light-triggered micelles for fast controlled drug release in deep tissue, Biomaterials 34 (2013) 6272–6283.
[13] P.T. Burks, J.V. Garcia, R. GonzalezIrias, J.T. Tillman, M. Niu, A.A. Mikhailovsky, J. Zhang, F. Zhang, P.C. Ford, Nitric oxide releasing materials triggered by near-infrared excitation through tissue filters, J. Am. Chem. Soc. 135 (2013) 18145–18152.
[14] J.V. Garcia, F. Zhang, P.C. Ford, Multi-photon excitation in uncaging the small molecule bioregulator nitric oxide, Philos. T. Roy. Soc. A 371 (2013) 20120129.
[15] A.D. Ostrowski, B.F. Lin, M.V. Tirrell, P.C. Ford, Liposome encapsulation of a photochemical NO precursor for controlled nitric oxide release and simultaneous fluorescence imaging, Mol. Pharm. 9 (2012) 2950–2955.
[16] J.R. Hwu, C.S. Yau, S.-C. Tsay, T.-I. Ho, Thermal- and photo-induced transformations of *N*-aryl-*N*-nitrosohydroxylamine ammonium salts to azoxy compounds, Tet. Lett. 38 (1997) 9001–9004.
[17] T.A. Alston, D.J. Porter, H.J. Bright, Generation of nitric oxide by enzymatic oxidation of *N*-hydroxy-*N*-nitrosamines, J. Biol. Chem. 260 (1985) 4069–4074.
[18] NTP, Report on Carcinogens. Department of Health and Human Services, Public Health Service., Research Triangle Park, NC: U.S. (2014).
[19] L.K. Keefer, Fifty years of diazeniumdiolate research: from laboratory curiosity to broad-spectrum biomedical advances, ACS Chem. Biol. 6 (2011) 1147–1155.
[20] R.J. Singh, N. Hogg, J. Joseph, B. Kalyanaraman, Photosensitized decomposition of S-nitrosothiols and 2-methyl-2-nitrosopropane: possible use for site-directed nitric oxide production, FEBS Lett. 360 (1995) 47–51.
[21] G.R. Buettner, In the absence of catalytic metals ascorbate does not autoxidize at pH 7: ascorbate as a test for catalytic metals, J. Biochem. Biophys. Methods 16 (1988) 27–40.
[22] A.E. Alegria, F.J. Dejesus-Andino, P. Sanchez-Cruz, Quinone-enhanced sonochemical production of nitric oxide from s-nitrosoglutathione, Ultrason. Sonochem. 16 (2009) 190–196.
[23] C.G.M. Millar, C. Thiemermann, Carboxy-PTIO, a scavenger of nitric oxide, selectively inhibits the increase in medullary perfusion and improves renal function in endotoxemia, Shock 18 (2002) 64–68.
[24] N. Hogg, Detection of nitric oxide by electron paramagnetic resonance spectroscopy, Free Radical Biol. Med. 49 (2010) 122–129.
[25] T.D. Oury, L. Tatro, A.J. Ghio, C.A. Piantadosi, Nitration of tyrosine by hydrogen peroxide and nitrite, Free Radical Res. 23 (1995) 537–547.
[26] I. Fridovich, Superoxide dismutase: an enzymatic function for erythrocuprein, J. Biol Chem. 244 (1969) 6049–6055.
[27] I. Fridovich, in: R.A. Greenwald (Ed.), Handbook of Methods for Oxygen Radical Research, CRC Press, Boca Raton, 1985, pp. 51–53.
[28] T. Akaike, M. Yoshida, Y. Miyamoto, K. Sato, M. Kohno, K. Sasamoto, K. Miyazaki, S. Ueda, H. Maeda, Antagonistic action of imidazolineoxyl N-oxides against endothelium-derived relaxing factor/: bul. NO (nitric oxide) through a radical reaction, Biochemistry (Moscow) 32 (1993) 827–832.
[29] E.F. Ullman, J.H. Osiecki, D. Boocock, R. Darcy, Stable free radicals: X. Nitronyl nitroxide monoradicals and biradicals as possible small molecule spin labels, J. Am. Chem. Soc. 94 (1972) 7049–7059.
[30] A.E. Alegria, Y. Inostroza, A. Kumar, Photosensitized oxidation of hypoxanthine and xanthine by aluminum phthalocyanine tetrasulfonate role of the alkylating quinone 2,5-dichloro-diaziridinyl-1, 4-benzoquinone, Photochem. Photobiol. 84 (2008) 1583–1588.
[31] P. Engst, P. Kubát, M. Jirsa, The influence of D_2O on the photophysical properties of meso-tetra (4-sulphonatophenyl) porphine, photosan III and

tetrasulphonated aluminium and zinc phthalocyanines, J. Photochem. Photobiol. A Chem. 78 (1994) 215–219.
[32] W.A. Pryor, R. Cueto, X. Jin, W.H. Koppenol, M. Ngu-Schwemlein, G.L. Squadrito, P.L. Uppu, R.M. Uppu, A practical method for preparing peroxynitrite solutions of low ionic strength and free of hydrogen peroxide, Free Radic. Biol. Med. 18 (1995) 75–83.
[33] P. Sanchez-Cruz, F. Dejesus-Andino, A.E. Alegria, Roles of hydrophilicities and hydrophobicities of dye and sacrificial electron donor on the photochemical pathway, J. Photochem. Photobiol. A Chem. 236 (2012) 54–60.
[34] D.R. Duling, Simulation of multiple isotropic spin-trap EPR spectra, J. Magn. Reson. 104 (1994) 105–110.
[35] J.A. Pedersen, Handbook of EPR Spectra from Quinones and Quinols, CRC Press, Boca Raton, FL, 1985.